PHYSICAL REVIEW B VOLUME 17, NUMBER 2 15 JANUARY 1978

Mutual drag effect in the magnetoresistivity of antimony

C. L. Tsai,* D. Waldorf, K. Tanaka,† and C. G. Grenier
Department of Physics and Astronomy, Louisiana State University, Baton Rouge, Louisiana 70893
(Received 2 May 1977)

Isothermal and adiabatic magnetoresistivities of an antimony single crystal have been determined in the temperature range 1.2–4.2 °K. The weak temperature dependence in the magnetoresistivities and the difference between the isothermal and adiabatic values are ascribed to the presence of the carrier-phonon mutual drag effect in the magnetoresistance. A simplified model of mutual drag in semimetals based on the fact that both carriers and phonons drift with almost the same transverse velocity was adapted. The observed values of mutual drag efficiency and electron-phonon interaction were consistent with those obtained from other transport measurements.

I. INTRODUCTION

The magnetoresistivity of semimetals, such as Bi and Sb, has been the subject of previous investigations.[1-7] In the present study we will direct our attention to the rather weak temperature dependence exhibited by the magnetoresistance of antimony in the helium temperature range.[8] Since such behavior seems to suggest that the electron-phonon scattering is either almost nonexistent or very inefficient in high magnetic field, it is thought that the strong electron-phonon mutual drag existing in the magnetoresistivity of antimony could be responsible for this effect. In the theory of the electron-phonon drag[9-13] phenomena, the relevant point to our investigation is summarized in the theoretical conclusion of Kagan[10]: "In the case of compensated metals with closed Fermi surfaces, the magnetic field itself produces a unified drift of the electron and holes, which in turn stimulates phonon drift. The stronger the phonon dragging the less effective the scattering and the larger the transverse resistance. Thus, dragging can manifest itself in the magnetoresistance of all metals with closed Fermi surfaces."

Current usage seems to designate drag phenomena as simple or mutual. The former, as the term implies, refers to the transfer of momentum from, say, electrons to phonons by electron-phonon interaction. The latter term seems to be associated with the idea that carriers interact with themselves through their mutual interaction with the phonons. Thus when electrons drift in response to an electric field, they drag phonons with them and any effect arising directly from this phonon drift will be referred to as a simple drag effect. For example, simple drag of phonons by carriers contributes significantly to the Ettingshausen effect. Now when the simple drag gives the phonons a drift velocity, the processes of momentum transfer between phonons and electrons will be affected and any alteration in *electronic* properties arising from this phonon drift is regarded as a mutual drag effect. For example, the transverse drift of phonons (Ettingshausen effect) produces changes in the magnetoresistivity by altering the scattering of carriers. Similarly when a longitudinal temperature gradient is applied to a Sb crystal in high magnetic field, the phonons, of course, drift in the direction of the gradient and thereby transfer momentum to the carriers, which are obliged by the applied magnetic field to drift transversely to both the temperature gradient and the magnetic field. This gives rise to a simple drag contribution to the Nernst-Ettingshausen effect and a mutual drag effect on the thermal resistance.

The experimental procedure and the results are given in Sec. II. In Sec. III a simplified drag model is developed for the case of antimony. Information obtained from the adiabatic and isothermal magnetoresistivities is used with the model to yield information about the mutual drag and the contribution of electron-phonon scattering to the magnetoresistivity. Further, information concerning drag and electron-phonon scattering obtained from other transport properties are also compared with the present data.

II. EXPERIMENTAL PROCEDURE AND RESULTS

The monocrystalline sample, No. 17 of Ref. 6 was used in this study. It was shaped by a spark cutter from a pure antimony ingot grade 69.[15] The dimensions of this sample are about 3×2.8×30 mm. The sample surfaces were lapped on No. 600 emery paper, electropolished, then subjected to a short etching. For such samples the surface currents were greatly diminished and a reasonable correction could be applied.[16] The long dimension of this sample, that is, the current direction, is parallel to the bisectrix axis which is denoted as x or 1 axis. The lateral faces are perpendicular to the

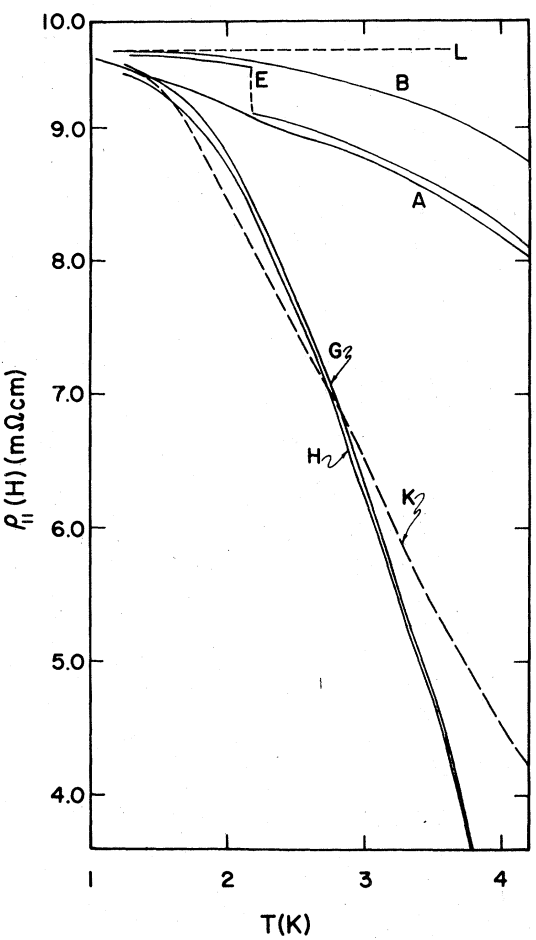

FIG. 1. Magnetoresistivity of antimony at 20 kG as a function of temperature: Adiabatic magnetoresistivity ρ_{11}^{a}, curve A; isothermal ρ_{11}, curve B. The experimental ρ_{expt} value, curve E, shows a step variation at the λ point of helium, with almost adiabatic behavior in the He I bath and almost isothermal behavior in the He II region. The resistivity zero-temperature limit ρ_{11}^{a} is shown as the broken line L. Curve K is obtained from the zero-field resistivity value by application of Kohler's rule. Curve G gives σ_{ep}^{-1} as obtained from Eq. (12). Curve H, same as G, but corresponds to the adiabatic σ_{ep}^{a} case. Curves A, B, L, E have not been corrected for surface current. Curves K, G, H have been properly modified to include surface effects.

binary axis (y or 2) and to the trigonal axis (z or 3) which is the direction of the applied magnetic field H. Under such conditions the bulk transport coefficients can be reduced by symmetry to a relatively simple form.

The electric current, sufficient to give a measured longitudinal dc potential difference of ~100 μV, was usually about 1 to 5 mA depending on the field H. The potential measurements for this investigation were made with a Rubicon potentiometer using a 147 Keithley nanovoltmeter as a null detector.

The sample was mounted in a cryostat used for thermal conductivity measurement. The adiabatic condition was obtained by evacuating the sample chamber so that no transverse heat current could flow. (The effect of longitudinal heat currents was eliminated by reversing current and magnetic field.) Measurements of the Ettingshausen effect were taken simultaneously with the adiabatic magnetoresistivity. Adiabatic conditions were also used in the measurement of the thermal resistivity and Nernst-Ettingshausen effect. The introduction of liquid helium into the sample chamber did not permit the direct measurement of the isothermal resistivity because of the low thermal conductance of liquid helium I in one hand and the Kapitza resistance between the sample and the helium II liquid bath in the other hand. The isothermal magnetoresistivity is estimated instead by applying a correction term to the measured adiabatic resistivity,[6] which is readily determined from the measured values for the Ettingshausen, Nernst-Ettingshausen effects, and the thermal conductivity. Isothermal magnetoresistivity can, in principle, be measured directly in a "Corbino geometry" experiment,[17] which allows for a circular unimpeded Ettingshausen heat flow. But this geometry does not allow for an adiabatic measurement and there exist difficulties in transposing results from this geometry (Corbino disk) to the presently used geometry (slab sample).

The measured values of magnetoresistivity are shown in Fig. 1 as a function of temperature for $H = 20$ kG. Curve A represents the measured adiabatic magnetoresistivity and curve B represents the isothermal resistivity as determined after correcting for the Ettingshausen heat contribution. Curve E, the magnetoresistivity as measured in the liquid helium bath, displays nearly adiabatic behavior in the He I bath and a not quite isothermal behavior in the liquid He II temperature range. The zero-temperature extrapolated value for the magnetoresistivity is shown as the broken line L. The other curves K, G, H are derived from theoretical considerations and will be described in the discussion.

The most striking feature is the very weak temperature dependence of the isothermal resistivity as compared with some of the qualitative expectations. Curve K, for example, which is obtained from simple application of Kohler's rule using measured zero-field resistivity, shows a much larger temperature dependence. Near 2 °K, the expected temperature contribution is hardly 5% of that expected from Kohler's approximation.

III. DISCUSSION

A. Drag equation

The coupled Boltzmann equations for carriers and phonons are given by[12]

$$\left(\frac{\partial f_{\vec{k}}^{\pm}}{\partial t}\right)_{\text{scatt}}+\left(\frac{\partial f_{\vec{k}}^{\pm}}{\partial t}\right)_{\text{diff}}+\left(\frac{\partial f_{\vec{k}}^{\pm}}{\partial t}\right)_{\text{field}}=0\,,$$
$$\left(\frac{\partial N_{\vec{q}}}{\partial t}\right)_{\text{scatt}}+\left(\frac{\partial N_{\vec{q}}}{\partial t}\right)_{\text{diff}}=0\,, \tag{1}$$

where $f_{\vec{k}}$ and $N_{\vec{q}}$ are the distribution functions for carriers and phonons, respectively. The superscripts "±" refer to carrier holes and electrons, respectively.

A standard approximation[18] is to assume that

$$f_{\vec{k}}^{\pm}=f_{\vec{k}}^{(0)\pm}-\vec{V}(\epsilon)^{\pm}\cdot(\vec{k}\hbar)\frac{\partial f_{\vec{k}}^{(0)\pm}}{\partial\epsilon}\,,$$
$$N_{\vec{q}}=N_{\vec{q}}^{(0)}-\vec{U}(\omega)\cdot(\vec{q}\hbar)\frac{\partial N_{\vec{q}}^{(0)}}{\partial(\hbar\omega_q)}\,, \tag{2}$$

where $f_{\vec{k}}^{(0)}$, $N_{\vec{q}}^{(0)}$ are the equilibrium distribution functions and $\vec{V}(\epsilon)$ and $\vec{U}(\omega)$ are the drift velocities of carriers of energy ϵ and of phonons of energy $\hbar\omega$, respectively. $\vec{k}$ and $\vec{q}$ are carrier and phonon wave vectors, k and q their absolute values.

In the presence of an electric field $\vec{E}$, a gradient of temperature $\vec{\nabla}T$ and magnetic field $\vec{H}$ integration may in principle be performed.[12] It is more easily expressed neglecting phonon polarization, assuming electron and phonon isotropy, a mean free path (mfp), and a quadratic energy dispersion for electrons and holes. An unscreened deformation-potential–electron-phonon interaction with a scattering frequency proportional to q is also assumed. Coupled equations in $\vec{V}(\epsilon)$ and $\vec{U}(\epsilon)$ may then be obtained.

$$\vec{V}^{\pm}(\epsilon)+(e^{\pm}l^{\pm}/cp^{\pm})[\vec{H}\times\vec{V}^{\pm}(\epsilon)]-(l^{\pm}/l_f^{\pm})\langle\vec{U}(x)\rangle_{\epsilon}^{\pm}=(l^{\pm}/p^{\pm})\{e^{\pm}\vec{E}-[(\epsilon-\xi^{\pm})/T]\vec{\nabla}T\}\,, \tag{3}$$

$$\vec{U}(\omega)=\frac{-L}{L^{+}}\int_{\epsilon^{+}(q/2)}^{\infty}\vec{V}^{+}(\epsilon)\frac{\partial f_{\vec{k}}^{(0)+}}{\partial\epsilon}d\epsilon-\frac{L}{L^{+}}\int_{\epsilon^{-}(q/2)}^{\infty}\vec{V}^{-}(\epsilon)\frac{\partial f_{\vec{k}}^{(0)-}}{\partial\epsilon}d\epsilon-\frac{Ls_g}{T}\vec{\nabla}T\,, \tag{4}$$

where $\langle U(x)\rangle_{\epsilon}^{\pm}$, the drift velocity of phonon averaged in the range of q between 0 and $2k$, is approximated by

$$\langle\vec{U}(x)\rangle_{\epsilon}^{\pm}=\frac{1}{J_5(x(\epsilon))}\int_0^{x^{\pm}(\epsilon)}\vec{U}(x)\frac{e^x x^5}{(e^x-1)^2}dx\,. \tag{5}$$

The Debye integrals $J_n(u)=\int_0^u[e^x x^n/(e^x-1)^2]\,dx$, $x=\hbar s_g q/K_BT$, and $x^{\pm}(\epsilon)=\hbar s_g 2k^{\pm}/K_BT$.

$l^{\pm}$ is the total mfp of the holes (electrons); $l_f^{\pm}$ is the mfp of the holes (electrons) due to scattering with phonons; $p^{\pm}$ is the momentum of holes (electrons) $p=\hbar k$; L is the total mfp of phonons; $L^{\pm}$ is the mfp of phonons due to scattering with holes (electrons); $k^{\pm}$ is the wave-vector magnitude of holes (electrons) of energy ϵ. s_g is the velocity of sound. Of particular interest are the limits of integration corresponding to the Fermi energy with

$$x(\xi^{\pm})=\hbar s_g 2k_F^{\pm}/K_BT=\Theta_{h,e}^{*}/T\,.$$

The index F corresponds to the Fermi energy, the subscript h (e) corresponds to holes (electrons), $\xi^{\pm}$ is the Fermi energy for holes (electrons), and $\Theta_{e,h}^{*}$ is the scattering Debye temperature of phonon by electrons (holes).

Though Eqs. (3) and (4) assume isotropic carrier distributions, they may be adapted to contain some of the selective anisotropic scattering of phonons and carriers. Thus, other Debye scattering temperatures are introduced as outlined in Sec. III B.

To solve Eqs. (3) and (4), an iteration method is used, wherein it is recognized that while the carrier drift velocities $\vec{V}^{\pm}$ are almost entirely limited by scattering from imperfections, the phonon drift velocity $\vec{U}$ is selectively limited mostly by the carrier-phonon interaction. The best iteration procedure will depend on the transport coefficient under consideration and on whether H is zero or not.

B. Selective electron-phonon interaction

In order to carry out the integration in Eq. (4), we must know L, $L^{\pm}$ for all $\vec{q}$. In the case of antimony at the temperatures of these experiments the interband and intervalley scattering processes are negligible leaving only electron-phonon normal processes and imperfection and boundary scattering of phonons. In the former case $\vec{k}'=\vec{k}+\vec{q}$, by which we have a limiting condition on $\vec{q}$. That is to say, if $|\vec{q}|$ is larger than the maximum diameter of the carrier pocket in the direction of $\vec{q}$ then carriers of that pocket will not scatter phonons of wave vector $\vec{q}$, nor $-\vec{q}$.[19] In the case of spherical carrier pockets, those phonons which are not scattered have $q>2k_F$; these are designated peripheral phonons. Those which can be scattered by carriers of the pocket ($q\leq 2k_F$) are called enclosed (en) phonons. Thus for a spherical Fermi pocket there exists in q space an image sphere having twice the dimensions of the carrier pocket. An ellipsoidal carrier pocket also yields in q space an ellipsoidal image having twice the size of the carrier pocket. For nonellipsoidal pockets such as occur in antimony, the image assumes a shape modeled on the carrier pocket but with nearly twice the caliper dimensions. Basically for a given direction of $\vec{q}$ any extremal caliper dimension of the carrier pocket (central or not) yields a radial dimension

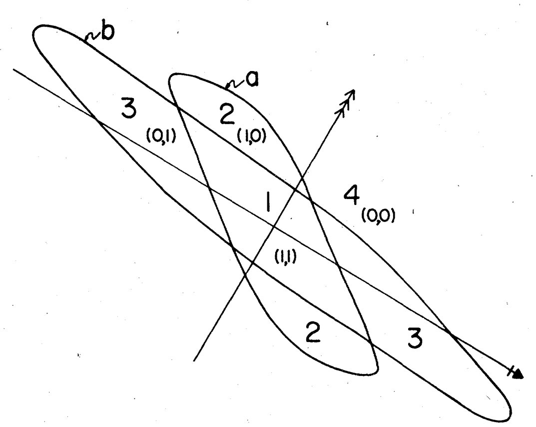

FIG. 2. Schematic two-pockets representation (Ref. 14) of the regions in q space, corresponding to different types of carrier-phonon scattering.

(central) of the phonon image. In antimony, corresponding to the three electron pockets there exist three image pockets which we label b_1, b_2, b_3, and corresponding to the three pairs of hole pockets there exist three image pockets which we label a_1, a_2, a_3.

In principle, we may divide phonon space into $2^6 = 64$ regions Rs where the index $s = (\alpha_1, \alpha_2, \alpha_3, \beta_1, \beta_2, \beta_3)$. For example $\alpha_1 = 1$ if Rs is inside the image a_1 and $\alpha_1 = 0$ if Rs is outside. For the region which is common to all regions $s = (1, 1, 1, 1, 1, 1)$, that is to say, phonons of this region can scatter carriers of any pockets. If at least one α and one β is different from zero then the phonons of that region can scatter both holes and electrons (this corresponds to the zero-field-compensated drag region). For peripheral phonons $s = (0, 0, 0, 0, 0, 0)$.

The schematic model for two pockets a and b is shown in Fig. 2. In region I, $s = (1, 1)$, phonons are scattered by holes and electrons. In region II, $s = (1, 0)$, phonons are scattered by holes only. In region III, $s = (0, 1)$, phonons are scattered by electrons only. In region IV, $s = (0, 0)$, phonons are not scattered by any of the carriers.

In order to use Eqs. (3) and (4) the anisotropic situation is approximated by spherical regions in q space characterized by a single parameter q_s^*, which in conforming to the Debye picture is given by $\hbar s_g q_s^*/k_B = \Theta_s^*$. For region I, $s = (1, 1)$ we have for the spherical approximation, the parameter Θ_1^*. Likewise we can make another spherical approximation for the sum of region I and region II, that is, $s = (1, \beta)$; thus giving the parameter $\Theta_2^* (= \Theta_h^*)$. For regions I and III, $s = (\alpha, 1)$ and $\Theta_3^* (= \Theta_e^*)$. Finally, for the region inside IV we have the parameter Θ_4^*.

The extension from the schematic two-pocket model to the six-pocket model can also yield a spherical approximation; the determination of the parameters will to some extent depend upon the transport coefficient in question. In an attempt to generalize the results of the schematic two-pocket model we will divide q space into four general regions.

The first general region, in the narrow sense, is region I with $s = (1, 1, 1, 1, 1, 1)$ and in a broader sense region I′ which contains all s where at least one α and one β are simultaneously different from zero. Correspondingly we would define a scattering Debye temperature which may vary between two values Θ_1^* and $\Theta_{1'}^*$ (zero-field-compensated drag region).

The second general region would be limited in the narrow sense as region II made of all s such that a given α is equal to one, the other coefficients taking any value (excluding all region s belonging to I or I′). In the broader sense it can be defined as region II′ where instead of *a given* $\alpha = 1$ (as in II) we have *at least one of the* $\alpha = 1$. Correspondingly $\Theta_{2'}^* > \Theta_2^*$ and one recognizes that Θ_2^* is simply Θ_h^* the scattering Debye temperature corresponding to one hole pocket ($\Theta_{2'}^*$ will correspond to the composite image associated with the three pairs of hole pockets).

The third region is defined similarly as the second region and relates to the electron scattering.

The fourth region corresponds to the peripheral phonons with $s = (0, 0, 0, 0, 0, 0)$ and a corresponding scattering temperature Θ_4^*.

C. Isothermal magnetoresistance ($\nabla T = 0$)

With the field $\vec{H}$ in the z direction, and $\vec{E}$ in the x direction, the first iteration of Eq. (3), using $\vec{U}(x) = 0$ gives, under the high-field condition,

$$\vec{V}^{\pm}(\epsilon) = \left(\left(\frac{c}{H}\right)^2 \frac{p^{\pm}}{e^{\pm} l^{\pm}} E,\ -\frac{cE}{H},\ 0\right). \qquad (6)$$

Substituting this value in Eq. (4) gives

$$\vec{U}(\omega_s) = \left(\left(\frac{c}{H}\right)^2 \frac{2E}{l^+}\left(2\sum_i \frac{\alpha_i p_F^+}{L_i^+ l^+} - \sum_i \frac{\beta_i p_F^-}{L_i^- l^-}\right) L_s,\ -\left(2\sum_i \frac{\alpha_i}{L_i^+} + \sum_i \frac{\beta_i}{L_i^-}\right)\frac{L_s c E}{H},\ 0\right). \qquad (7)$$

If we do not differentiate between the scattering by electrons of one pocket from another, then $L_i^- = L^-$; similarly $L_i^+ = L^+$ and L_s is given by

$$\frac{1}{L_s} = \frac{1}{L_R} + \left(2\sum \alpha/L^+ + \sum \beta/L^-\right). \qquad (8)$$

In this expression the term $1/L_R$, arising from other cause than electron-phonon scattering, is rather negligible except in region IV where electron-phonon scattering does not occur.

With $\gamma_s = L_s(2\sum\alpha/L^+ + \sum\beta/L^-)$ the U_y drag term in (7) is $-\gamma_s cE/H$ and since $L_s/L_R = 1-\gamma_s \ll 1$ one may neglect to a first approximation the effect due to the variation of γ_s from region to region and replace it by an average value $\bar{\gamma}$. Then the correction brought by substituting Eq. (7) in Eq. (3) yields the approximate (mutual) drag term

$$\delta\vec{V}^{\pm} \simeq \left(-\left(\frac{c}{H}\right)^2 \frac{\bar{\gamma}p^{\pm}E}{e^{\pm}l_f^{\pm}}, 0, 0\right). \tag{9}$$

Self-consistency by more iteration could be achieved, but is not necessary here, and unwarranted because of the approximations already made.

The isothermal magnetoconductivity is then given by $\sigma_{11}^{\pm} = \sigma_{11\,\mathrm{imp}}^{\pm} + \sigma_{\mathrm{ideal}}^{\pm}$, i.e.,

$$\sigma_{11}(H) = n\left(\frac{c}{H}\right)^2 \left(\frac{p_F^+}{l_{\mathrm{imp}}^+} + \frac{p_F^-}{l_{\mathrm{imp}}^-} + \frac{(1-\bar{\gamma})p_F^+}{l_f^+} + \frac{(1-\bar{\gamma})p_F^-}{l_f^-}\right), \tag{10}$$

where n is the total number of holes (or electrons) per unit volume. For a perfect mutual drag, the coefficient $\bar{\gamma} = 1$ and the magnetoresistivity[20] is temperature independent and equal to its zero temperature limit (curve L, Fig. 1).

$$\rho_{11}^0 \approx \{\sigma_{11\,\mathrm{imp}}\}^{-1} = \frac{1}{n}\left(\frac{H}{c}\right)^2 \left(\frac{p_F^+}{l_{\mathrm{imp}}^+} + \frac{p_F^-}{l_{\mathrm{imp}}^-}\right)^{-1}. \tag{11}$$

The weak temperature dependence in the isothermal magnetoresistivity is associated with the term

$$\sigma_{\mathrm{ideal}} = n(1-\bar{\gamma})\left(\frac{p_F^+}{l_f^+} + \frac{p_F^-}{l_f^-}\right)\left(\frac{c}{H}\right)^2 = (1-\bar{\gamma})\sigma_{ep}, \tag{12}$$

whereby $(1-\bar{\gamma})$ is small but not zero.

D. Adiabatic magnetoresistance

Under the adiabatic conditions no transverse heat current can flow, and therefore a transverse temperature gradient ∇T_y (the longitudinal component ∇T_x is negligible) is generated, which should partially "turn off" the simple drag of phonons and thus yield a more efficient electron-phonon scattering. Since the Ettingshausen temperature gradient ∇T_y is small, one may simply superimpose its effect in Eq. (3) in order to obtain the modified drift component in the x direction $V_x^{\pm}(\xi^{\pm})$, and the corresponding adiabatic magnetoconductivity coefficient σ_{11}^a. The y component of the phonon drift becomes

$$U_y(\omega_s) = -\gamma_s \frac{E}{H/c} - L_s \frac{s_g}{T}\frac{\partial T}{\partial y}. \tag{13}$$

But since there is no heat flow in the y direction one has $\partial T/\partial y = -(\pi_{21}''/\lambda_g)E$ where π_{21}'' is the Ettingshausen coefficient and λ_g is the total (lattice) thermal conductivity.

However[21]

$$\pi_{21}'' = T\epsilon_{21}'' = [T/(H/c)](C_e + \tfrac{1}{3}\bar{\gamma}C_g^{\mathrm{en}}), \tag{14}$$

where C_e is the carrier's specific heat and $C_g^{\mathrm{en}} \simeq C_g(\Theta_4^*/T)$ is the specific heat of the enclosed phonons, i.e., all phonons except the peripheral phonons.

Then taking into account the added term in $\partial T/\partial y$ the solution of Eq. (3) yields an x component for the carrier drift velocity

$$e^{\pm}V_x^{\pm}(\epsilon) = \left(\frac{c}{H}\right)^2 \frac{p^{\pm}}{l^{\pm}}\left(-\frac{l^{\pm}}{l_f^{\pm}}\langle\gamma_s\rangle_\epsilon^{\pm}\right)E + \frac{c}{H}\left\{\frac{\epsilon-\xi^{\pm}}{T} + \frac{p^{\pm}}{l^{\pm}}\frac{s_g}{T}\langle L_s\rangle_\epsilon^{\pm}\right\}\frac{\pi_{21}''}{\lambda_g}E \tag{15}$$

where $\langle\gamma_s\rangle_\epsilon^{\pm}$ and $\langle L_s\rangle_\epsilon^{\pm}$ are averages of the same type as in Eq. (5).

When this value of V_x is used in the calculation of current, J_x, the conductivity takes the form

$$\sigma_{11}^{(a)\pm} = \{\sigma_{11\,\mathrm{imp}}^{\pm} + \sigma_{ep}^{\pm}(1-\bar{\gamma})\} + \left\{\sigma_{ep}^{\pm}\frac{H}{c}\frac{s_g}{T}\bar{L}_{h,e}\frac{\pi_{21}''}{\lambda_g} + \frac{c}{H}C_e^{\pm}\frac{\pi_{21}''}{\lambda_g}\right\}, \tag{16}$$

where we have made use of the relation $1/l^{\pm} = 1/l_{\mathrm{imp}}^{\pm} + 1/l_f^{\pm}$. The averages

$$\bar{\gamma}_{h,e} = \langle\gamma_s\rangle_{\xi^{\pm}}^{\pm} = \frac{1}{J_5(\Theta_{h,e}^*/T)}\int_0^{\Theta_{h,e}^*/T}\frac{\gamma_s x^5 e^x\,dx}{(e^x-1)^2}$$

and

$$\bar{L}_{h,e} = \langle L_s\rangle_{\xi^{\pm}}^{\pm} = \frac{1}{J_5(\Theta_{h,e}^*/T)}\int_0^{\Theta_{h,e}^*/T}\frac{L_s x^5 e^x\,dx}{(e^x-1)^2}$$

can be regarded as independent of the limit of integration[22] and characteristic of all enclosed phonons $\bar{\gamma}_h = \bar{\gamma}_e = \bar{\gamma}^{\mathrm{en}} = \bar{\gamma}$ (likewise for $\bar{L}$). The first bracket corresponds to $\sigma_{11}^{\pm}$ the isothermal conductivity as in Eq. (10). The second term gives for $\sigma_{11}^a - \sigma_{11}$ the quantity

$$\frac{\pi_{21}''}{\lambda_g}\left(\frac{c}{H}C_e + \frac{H}{c}\sigma_{ep}\frac{s_g\bar{L}}{\lambda_g}\right)$$

which to a good approximation can be identified with $(\pi_{21}''/\lambda_g)\epsilon_{21}''$ so that from Eq. (14) $(H/c)\sigma_{ep}(\bar{L}s_g/\lambda_g) \simeq \frac{1}{3}\bar{\gamma}C_g^{\mathrm{en}}$. If we introduce $\frac{1}{3}Ls_gC_g^{\mathrm{en}} = \lambda_g^{\mathrm{en}}$, the contribution of enclosed phonons to lattice conduction, and $\lambda_g^{\mathrm{en}}/\bar{\gamma}$, the conduction of these phonons due to carrier scattering alone, one obtains

$$\left(\frac{H^2\sigma_{ep}}{c^2}\right)\frac{\lambda_g^{\mathrm{en}}}{\gamma} \approx \left(\frac{C_g^{\mathrm{en}}}{3}\right)^2 T, \tag{17}$$

an equation similar to this obtained by Ziman[23] for zero field $\{\rho_L W_e^{-1} = (n^2/e^2)(\frac{1}{3}C)^2 T\}$ relating the ideal resistivity ρ_L [in place of $\sigma_{ep}(H/c)^2(n/e)^2$] with the phonon heat conductivity due to carrier scattering W_e^{-1} (in place of $\lambda_g^{en}/\bar{\gamma}$).

It is interesting also to note that σ_{ep} (i.e., the undragged conductivity) not $(1-\bar{\gamma})\sigma_{ep}$ is the ideal conductivity which appears in this relation (17). When one expresses Eq. (16) in function of λ_g^{en} the corrective term appearing in the adiabatic conductivity takes the form

$$\sigma_{11}^{(a)} - \sigma_{11} = \frac{c}{H}\frac{\pi_{21}''}{\lambda_g}\left[C_e + \sigma_{ep}\left(\frac{H}{c}\right)^2 \frac{3\lambda_g^{en}}{TC_g^{en}}\right]. \qquad (18)$$

E. Comparison with experimental results

The primary experimental coefficient is the adiabatic conductivity $\sigma_{11}^{(a)}$. The isothermal-conductivity σ_{11} is determined from the relation $\sigma_{11} \approx \sigma_{11}^{(a)} - \pi_{21}''\epsilon_{21}''/\lambda_g$ with Ettingshausen π_{21}'', Nernst-Ettingshausen ϵ_{21}'', and thermal (lattice) conductivity λ_g coefficients measured separately. This conductivity σ_{11} is known rather accurately as well as $\sigma_{11\,\text{imp}}$ the limit of σ_{11}^{a} and σ_{11} as T tends to zero.

The ideal conductivity σ_{id} is obtained from $\sigma_{\text{id}} = \sigma_{11} - \sigma_{11\,\text{imp}}$; it is known rather precisely except in the low-temperature range where the uncertainty in the extrapolation to $T = 0$ yields a relatively large uncertainty in σ_{id}.

As shown in Eqs. (12) and (16), $\sigma_{\text{id}} = (1-\bar{\gamma})\sigma_{ep}$ is reduced due to drag by the coefficient $1-\bar{\gamma}$ as compared to σ_{ep} the magnetoconductivity due to electron–"undragged"-phonons interaction. In order to obtain an estimate of the magnitude of this effect one needs to determine separately the values of σ_{ep} and $\bar{\gamma}$.

A term involving σ_{ep} appears in $\sigma_{11}^{(a)} - \sigma_{11}$ Eq. (18) and can be used to estimate the σ_{ep} value. An estimate for $\bar{\gamma}$ can be obtained from the directed analysis[21] of the coefficient $\pi_{21}'' = (cT/H)(C_e + \frac{1}{3}\bar{\gamma}C_g^{en})$.

Also from Eq. (17) the value $\bar{\gamma}\sigma_{ep} = (c/H)^2(T/\lambda_g^{en})(\frac{1}{3}\bar{\gamma}C_g^{en})^2$ can be estimated, since $\frac{1}{3}\bar{\gamma}C_g^{en}$ is directly determined from the ϵ_{21}'' or π_{21}'' coefficient analyses and λ_g^{en} can be extracted from the lattice conductivity.[21]

The best fit for these different quantities yield a value $\bar{\gamma} \approx 0.93 \pm 0.02$.[24] The mutual drag therefore reduces the ideal conductivity by nearly 20 times from the σ_{ep} expected value. The value for σ_{ep} is given in Fig. 3 where it is shown to exhibit the Gruneisen T^5 law in the low-temperature range. A corresponding composite value for the magnetoresistance "without drag" is also shown in Fig. 2, with curve G corresponding to the isothermal case and curve H to the adiabatic case.

To proceed to the analysis of σ_{ep} one may use the expression (12)

$$\sigma_{ep} = n(c/H)^2\,(p_F^+/l_f^+ + p_F^-/l_f^-)$$

with

$$\frac{1}{l_f^\pm} = \frac{9\pi h^2 \mathcal{E}_{h,e}^2 N n a^\pm}{8\rho s_g \xi_\pm^2 p_F^\pm \nu^\pm}\left(\frac{\Theta_D}{\Theta_{h,e}^*}\right)^2\left(\frac{T}{\Theta_D}\right)^5 J_5\left(\frac{\Theta_{h,e}^*}{T}\right), \qquad (19)$$

where $\mathcal{E}_{h,e}$ is the deformation potential for holes (electrons), N the number of atoms per unit volume, ρ the mass density, Θ_D the Debye temperature, $a^\pm$ an anisotropy factor,[25] $\nu^+ = 6$ and $\nu^- = 3$ the number of hole and electron pockets, respectively.

In antimony since $l_f^- \ll l_f^+$ we may to a first approximation consider only the electron contribution $\sigma_{ep} \approx \sigma_{ep}^-$. With this approximation the values obtained for the deformation potential and the effective Debye scattering temperature for electrons are

$$\mathcal{E}_e \approx 2.9 \text{ eV} \quad \text{and} \quad \Theta_e^* \approx 26\ ^\circ\text{K}.$$

The value for the deformation potential is in very good agreement with that obtained by Gantmaker and Dolgopolov[26] from the radio-frequency size-effect mean-free-path measurement. It is also in good agreement with the value deduced from the electronic part of the thermal magnetoresistance.[7]

The value for Θ_e^* is somewhat smaller than 28.5 °K, the value obtained from the electronic part of the thermal magnetoresistance,[7] and smaller than 30.8 °K the estimate from the size $(k_{F(\text{av})})$ of the electron pockets. It is to be pointed out that the determination of Θ_e^* is affected firstly by approximating γ_s to a constant $\bar{\gamma}$ and secondly by

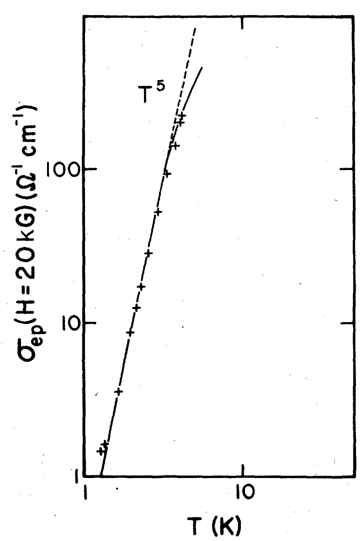

FIG. 3. Value of σ_{ep} (corrected for surface current) is shown as a function of temperature for $H = 20$ kG, and it is seen to exhibit the expected low temperature T^5. But the experimental and extrapolation errors are too large to trust these results to be a firm confirmation of the T^5 behavior.

the neglect of the hole contribution σ_{ep}^{+}. This later contribution may partly explain the apparent smaller value for Θ_e^*.

The values obtained here for $\bar{\gamma}$, $\mathcal{E}_e$, and Θ_e^* are in general agreement with those determined from other transport effects.[27]

General qualitative agreement is also obtained by application of Kohler's rule.[28] If it is assumed that the scattering is not affected by the magnetic field $\rho(H,T)/\rho(0,T)=F(H/\rho(0,T))$ and the value obtained for $\rho(H,T)$ using the zero field $\rho(0,T)$ value is shown as curve K in Fig. 1. The zero-field conduction corresponds to a situation of compensated drag, i.e., close to a nondrag conduction and the estimated "Kohler's value" for resistivity, matches more closely the nondrag values (curve G) than the isothermal experimental value (curve B).

When the results of magnetoresistance are compared with those of thermal magnetoresistance[7] some interesting points can be made. As pointed out above, the unified drift of carriers and phonons under the condition of isothermal magnetoresistance measurement reduces the efficacy of electron-phonon scattering because of the reduction of momentum transfer between the two systems. But the conditions under which thermal magnetoresistance is measured on one hand does not yield the same unified drift and on the other hand this effect depends on energy transfer during the scattering which even under drag condition is a more efficient scattering than that which depends on momentum transfer. Assuming a maximum efficiency, the experimental electronic thermal magnetoresistance corresponding to phonon scattering $\lambda_{e(\mathrm{ideal})} = \lambda_{ep}$, yields the values $\mathcal{E}_e = 3.00$ eV and $\Theta_e^* \approx 28.5$ °K in very good agreement with the determined σ_{ep} value. In other words, the contribution to the electrical and thermal magnetoconductivity which are due to the electron-phonon scattering can be expressed by

$$\sigma_{\mathrm{expt}} = (1-\bar{\gamma}_\sigma)\sigma_{ep}\,, \quad \lambda_{\mathrm{expt}} = (1-\bar{\gamma}_\lambda)\lambda_{ep}$$

with $\bar{\gamma}_\sigma$ close to unity (strong effect of drag) and $\bar{\gamma}_\lambda$ close to zero (unaffected by drag) as σ_{ep} and λ_{expt} yield the same electron-phonon scattering parameters.

A weak temperature dependence of the magnetoconductivity of Bi is also observed[29] which is not due to drag since $\bar{\gamma}$ is expected to be small. In Bi the phonons are scattered primarily by the boundaries. Although the electron-phonon scattering is "efficient" its contribution to the magnetoconductivity is negligible for other reasons and Kohler's rule applies for this case.

In conclusion, the weak temperature dependence of the magnetoresistance of antimony at low temperatures is a direct consequence of the nearly unified drift of the electrons, holes and phonons. Analysis of the adiabatic situation, and numerical determination of transport parameters such as electron-phonon scattering efficiency, deformation potential, Debye scattering temperature are in agreement with those determined from other effects.[27]

We would like to acknowledge Dr. R. C. Crosby for his help during the early part of this study.

---

*Present address: Dept. of Physics, Illinois Institute of Technology, Chicago, Ill. 60616. In partial fulfillment of Ph.D. degree.

†Present address: Dept. of Electronic Engineering, Yamaguchi University, Ube, Yamaguchi, Japan.

[1]No attempt will be made here to give a comprehensive list of references. References 2–7 are related to this subject for the case of antimony. Other relevant references can be found in those articles.

[2]C. G. Grenier, J. R. Long, J. M. Reynolds, and N. H. Zebouni, *Low Temperature Physics* (Plenum, New York, 1965); J. R. Long, C. G. Grenier, and J. M. Reynolds, Phys. Rev. 140, A187 (1965).

[3]S. J. Freedman and H. J. Juretchke, Phys. Rev. 124, 1379 (1961); S. Epstein and H. J. Juretchke, *ibid.* 129, 1148 (1963).

[4]M. C. Steele, Phys. Rev. 99, 1751 (1955).

[5]Yu. A. Bogod, B. I. Verkin, and V. B. Krasovitskii, Zh. Eksp. Teor. Fiz. 61, 275 (1971) [Sov. Phys.-JETP 34, 142 (1972)]; Yu. A. Bogod and V. B. Krasovitskii, Zh. Eksp. Teor. Fiz. 63, 1036 (1972) [Sov. Phys.-JETP 36, 544 (1973)].

[6]C. L. Tsai, D. L. Waldorf, K. Tanaka, and C. G. Grenier, Phys. Rev. B 15, 4968 (1977).

[7]C. L. Tsai, dissertation (Louisiana State University, 1976) (unpublished).

[8]The point was noted in Ref. 2. It is also noted in Ref. 5 (1972) that the mean free path determination from the temperature dependence is in disagreement with its determination from the size dependence.

[9]See, for example, L. E. Gurevich and I. Ya. Korenblit, Fiz. Tverd. Tela 9, 1195 (1967) [Sov. Phys.-Solid State 9, 932 (1967)].

[10]Yu. Kagan and Y. N. Flerov, Pis'ma Zh. Eksp. Teor. Fiz. 20, 621 (1974) [JETP Lett. 20, 284 (1974)].

[11]F. W. Sheard, J. Phys. F 3, 1963 (1973).

[12]J. M. Ziman, *Electrons and Phonons* (Oxford U.P., London, 1960).

[13]A. H. Wilson, *The Theory of Metals,* 2nd ed. (Cambridge U.P., Cambridge, 1954).

[14]Both pockets shown here are modeled after the Fermi-surface determination by R. A. Herrod, C. A. Gage, and R. G. Goodrich, Phys. Rev. B 4, 1033 (1971).

[15]Grade 69 zone refined bar, Cominco Products, Inc.,

Spokane, Washington.

[16]More detailed information about the sample treatment and experimental procedure is given in Refs. 6 and 7.

[17]O. M. Corbino, Phys. Z. 12, 561 (1911); see, for example, *Methods of Experimental Physics* (Academic, New York, 1959), Vol. 6 B.

[18]This approximation is used by Gurevich (Ref. 9) among others.

[19]Since we have $T \ll T_F$, the Ziman cutoff function is practically a step function. See J. M. Ziman, Philos. Mag. 1, 191 (1956).

[20]In the present case the Hall conductivity is negligible so that with $\sigma_{12} \ll \sigma_{11}$ the magnetoresistivity equals the reciprocal of the magnetoconductivity $\rho_{11} \approx \sigma_{11}^{-1}$.

[21]R. S. Blewer, N. H. Zebouni, and C. G. Grenier, Phys. Rev. 174, 700 (1968).

[22]If $\bar{\gamma}$ and $\bar{L}$ are not supposed constant, the term $\sigma_{ep}^{+}(1-\bar{\gamma})$ is replaced approximately by $\sigma_{ep\,\mathrm{I}}^{+}(1-\bar{\gamma}_{\mathrm{I}})+(\sigma_{ep\,\mathrm{II}}^{+}-\sigma_{ep\,\mathrm{I}}^{+})(1-\bar{\gamma}_{\mathrm{II}})$ and $\sigma_{ep}^{+}\bar{L}$ is replaced by a similar term. Indices I, II refer to region of scattering characterized by Θ_1^* (or $2k_{F1}$) and Θ_2^* (or $2k_{Fh}$), with $\sigma_{ep\,\mathrm{I}}^{+}=n_{\mathrm{I}}=(c/H)^2 p_{F\mathrm{I}}/l_{f\,\mathrm{I}}^{+}$ and

$$1-\bar{\gamma}_{\mathrm{I}}=J_5(\Theta_1^*/T)^{-1}\int_0^{\Theta_1^*/T}(1-\gamma_{\mathrm{I}})\frac{x^5 e^x\,dx}{(e^x-1)^2}$$

with

$$1-\gamma_{\mathrm{I}}=\frac{1}{L_R}\left(\frac{1}{L_R}+2\sum\alpha\Big/L^{+}+\sum\beta\Big/L^{-}\right)^{-1},$$

where $\sum\alpha$ and $\sum\beta$ both between 1 and 3 and $1-\gamma_{\mathrm{II}}=(1/L_R)(1/L_R+2\sum\alpha/L^{+})$ with $\sum\alpha$ fudged between 1 and 3.

[23]See, for example, J. M. Ziman, Ref. 12, p. 321.

[24]Efficient drag $\bar{\gamma}\approx 1$ is well confirmed mostly through Nernst-Ettingshausen data, see Refs. 2, 17; also M. S. Bresler and N. A. Red'ko, Zh. Eksp. Teor. Fiz. 62, 1867 (1972) [Sov. Phys.-JETP 35, 973 (1972)]; S. K. Bansal and V. P. Buggal, J. Phys. Chem. Solids 35, 979 (1974).

[25]G. N. Rao, N. H. Zebouni, C. G. Grenier, and J. M. Reynolds, Phys. Rev. 133, A141 (1964). The values $a^{+}=1.6$, $a^{-}=2.6$ pertain to electron-impurity scattering. Note that there is an error of sign in the Hall effect in this article and that in Sec. III electron and hole could be reversed. The value obtained for $\mathcal{E}_e$ will depend on the value chosen for a^{-}. Here the value $\mathcal{E}_e=2.9$ eV corresponds to $a^{-}=2.6$.

[26]V. F. Gantmaker and V. T. Dolgopolov, Zh. Eksp. Teor. Fiz. 60, 2260 (1971) [Sov. Phys.-JETP 33, 1215 (1971)], give a value $|\Delta^{\mathrm{el}}|=2.9$ eV.

[27]General correlations in the contribution of drag in the different transport coefficients of antimony will be published at a later date.

[28]See, for example, A. H. Wilson, Ref. 8, p. 315; or J. M. Ziman, Ref. 12, p. 491.

[29]J. R. Sybert, dissertation (Louisiana State University, 1961) (unpublished).